18TH WORLD CONFERENCE ON EARTHQUAKE ENGINEERING
WCEE2024
MILAN

MILAN, ITALY
30TH JUNE - 5TH JULY 2024
www.wcee2024.it

LIFE-CYCLE ENVIRONMENTAL IMPACTS OF SEISMIC RETROFIT MEASURES: A CASE STUDY ON REINFORCED CONCRETE JACKETING IN ITALY

K. Aljawhari[1,2], R. Gentile[2] & C. Galasso[2]

[1]University School for Advanced Studies (IUSS) Pavia, Pavia, Italy

[2]University College London (UCL), London, United Kingdom

Abstract: *The increasing awareness of building sustainability in earthquake-prone areas constitutes a motive for investigating the influence of common seismic risk mitigation measures, such as structural retrofit, from a life-cycle environmental perspective. Accordingly, this study sheds light on the effects of reinforced concrete (RC) jacketing, a common retrofit strategy, on the life-cycle environmental impacts generated throughout the service life of a non-ductile RC frame constructed in Italy before the 1970s. Various layouts and configurations of retrofit configurations are developed to represent different design choices. The environmental impacts are expressed in terms of embodied carbon, a parameter that measures the overall greenhouse gas emissions associated with the life stages of a system (e.g., manufacturing, construction, maintenance, disposal). The life-cycle embodied carbon includes the earthquake-induced emissions evaluated by characterising the seismic damage sustained by the structure and then converting it to embodied carbon using suitable consequence models. The other life-cycle component is the embodied carbon of retrofit intervention, for which a simplified expression that relies on the retrofit layout and geometric features is derived. Results show that the life-cycle embodied carbon of the as-built structure constitutes 70% of that related to initial construction. The use of RC jacketing could reduce this percentage to as low as 43%.*

1 Introduction

The severity of earthquake impacts in the past few decades (e.g., De Luca et al. 2018) has highlighted the importance of seismic risk mitigation measures aimed at enhancing community resilience and reducing the vulnerability of the physical environment. This becomes more relevant in countries with substantial portions of buildings that do not conform to modern building code requirements, making them susceptible to significant damage, even under moderate ground-shaking events. While substituting these buildings with code-compliant ones can bring a pronounced reduction of vulnerability, it is typically beyond the financial capabilities of public entities, in addition to the environmental concerns that might arise. Hence, it is recommended to enhance the performance of existing buildings via structural retrofitting using one or more strategies, such as adding shear walls/bracing (e.g., Miano et al. 2017; Gutiérrez-Urzúa and Freddi 2022) and encasing columns with steel or reinforced concrete (RC) jackets, or wrapping them with fibre-reinforced polymers.

One of the crucial aspects of structural retrofit is the selection of suitable strategies that achieve both seismic performance enhancement and economic feasibility, especially in building portfolios where public funds are very limited. Numerous past studies have investigated such issues. For example, Liel and Deierlein (2013) conducted a benefit-cost analysis (BCA) to assess the retrofit effectiveness for older RC frames by obtaining the ratio between the reduction in direct loss (repair costs) and the cost of retrofit. Other forms of BCA were also adopted (e.g., Cardone et al. 2019; Natale et al. 2021). Some studies adopted multi-criteria decision-making (MCDM) methods, enabling the selection of a suitable retrofit strategy by comparing alternatives against user-defined criteria (e.g., Caterino et al. 2008; Muntasir Billah and Shahria Alam 2014; Gentile and Galasso 2021; Gallo et al. 2022). This method also allows the consideration of non-quantitative decision criteria such as functional compatibility and level of disruption.

Selecting the best retrofit strategy among several alternatives has been extensively studied in the literature, but the earthquake consequences involved in the decision-making are typically the repair costs (direct losses) incurred due to the repair of physical damage. However, the increasing global emphasis on sustainability in earthquake-prone regions has shifted the research focus towards evaluating the environmental impacts (EIs) of seismic damage stemming from the repair needed to restore building components to their original condition (e.g., Welsh-Huggins and Liel 2018; Gonzalez et al. 2022).

Nevertheless, the available studies on the influence of seismic retrofit on building sustainability with respect to life cycle EIs are still limited. For instance, Menna et al. (2016) evaluated the EIs generated by different retrofit interventions on masonry buildings but did not consider those produced by seismic damage. Clemett et al. (2022) used MCDM to integrate the repair costs and EIs in the selection of a suitable retrofit strategy. An improved work was accomplished by Caruso et al. (2020, 2023), who proposed combining seismic retrofit with energy upgrade and then measuring the EIs of seismic damage and operational energy in MCDM. The retrofit strategies adopted by these studies did not include RC jacketing, although it is the most common in engineering practice. Moreover, only one configuration was considered for each strategy, which might not be the optimal solution offering the most significant reduction of life-cycle EIs.

Based on the above, the current study examines the life-cycle sustainability of a case-study reinforced concrete (RC) frame retrofitted using RC jacketing. This entails the EIs generated by the repair of seismic damage sustained by the frame during its service life, in addition to those resulting from retrofit interventions. A practical formula is developed to evaluate the latter component, which depends on the geometry of the building and RC jackets. Various geometric details and configurations of RC jacketing are considered to assess the capability of this retrofit strategy to reduce the life-cycle EIs and identify the optimal design.

This study is organised as follows: Section 2 describes the implemented methodology, including the design of retrofit strategy, derivation of fragility relationships, estimation of the EIs of seismic damage and retrofit intervention; Section 3 presents the results of life-cycle EIs for both the as-built and retrofitted configurations and highlights the increase of sustainability due to seismic retrofit; and Section 4 provides some conclusions.

2 Methodology

This study investigates the life-cycle EIs for a case-study RC frame retrofitted via RC jacketing using different layouts and geometric details. The adopted methodology incorporates the following steps: 1) identify a case-study building; 2) develop a numerical model to simulate its non-linear behaviour; 3) design the retrofit strategy with various layouts and geometries; 4) derive fragility relationships that define the exceedance probabilities of different damage levels; 5) characterise site-specific seismic hazard; 6) obtain the life-cycle EIs induced by seismic damage and those generated as a result of retrofit interventions; 7) assess the reduction of life-cycle EIs and explore their influence on the retrofit design optimisation.

2.1 Case-study Definition

An older five-storey residential RC frame with a height of 15 m and four bays of 4.5 m each in both horizontal directions, as depicted in Figure 1. This frame was designed by Aljawhari et al. (2022) to reflect those built in Italy before the 1970s (Rosti et al. 2021). Such buildings resist gravity loads only and are expected to perform poorly under ground shaking due to the lack of seismic provisions (e.g., high confinement, capacity design).

2.2 Retrofit via RC Jacketing

RC jacketing is one of the most common retrofit strategies, and it involves enhancing existing columns with cast-in-situ RC encasement (see Figure 2a), which improves confinement, ductility, and both shear and flexural strengths. The continuous column jacketing on two consecutive floors can upgrade the joint behaviour as well. The jacket thickness is governed by the size of longitudinal and transverse rebar, in addition to the required minimum cover (e.g., Priestley et al. 1996). The reader is referred to Aljawhari et al. (2022) for a full description of the material, geometric, and reinforcement details associated with this retrofit strategy.

2.3 Non-linear Numerical Modelling

The non-linear response of the as-built and retrofitted layouts of the case-study structure is simulated via 2D numerical models developed in a prior work by the authors (Aljawhari et al. 2022) using OpenSees (McKenna 2011). Structural components were modelled as beam-column elements with finite-length plastic hinges to address the flexural response. Shear springs were added in series to the structural elements to account for

potential shear mechanisms. The joint failure was also modelled. The RC jackets were treated as equivalent monolithic elements. Infill walls are not modelled for simplicity. A detailed explanation of the modelling strategy and selected non-linear materials is available in Aljawhari et al. (2022).

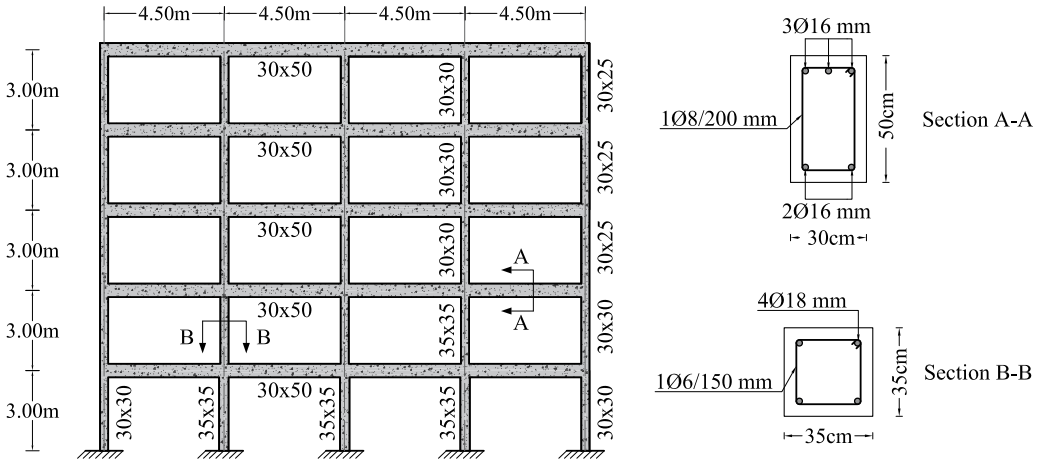

Figure 1. Geometry of the case-study building and representative rebar details.

2.4 Design of Retrofitted Configurations

The RC jacketing strategy was adopted to produce a large number of configurations (realisations) of retrofitted structures within in a previous study by the authors (Aljawhari et al. 2022). An iterative design procedure was implemented, in which the iterations vary with respect to detailing, geometric characteristics, and the number of retrofitted elements. This allowed an incremental improvement in seismic performance, which in turn was captured by measuring the displacement-based global ratio between capacity and life-safety seismic demand (CDR_{LS}) or simply the capacity-demand ratio (NZSEE 2017). The seismic demand was defined as a Type-1 response spectrum from Eurocode 8 (EN 1998-1 2004) with a peak ground acceleration of 0.30g, representing high seismicity. The CDR_{LS} value for each retrofitted configuration was eventually estimated using non-linear static (pushover) analysis combined with the capacity spectrum method (CSM) (ATC 1996). Figure 2b offers a schematic illustration of the CSM for the as-built structure, confirming that the demand spectrum substantially exceeds the capacity, with a $\mathrm{CDR_{LS}}$ equal to 42%.

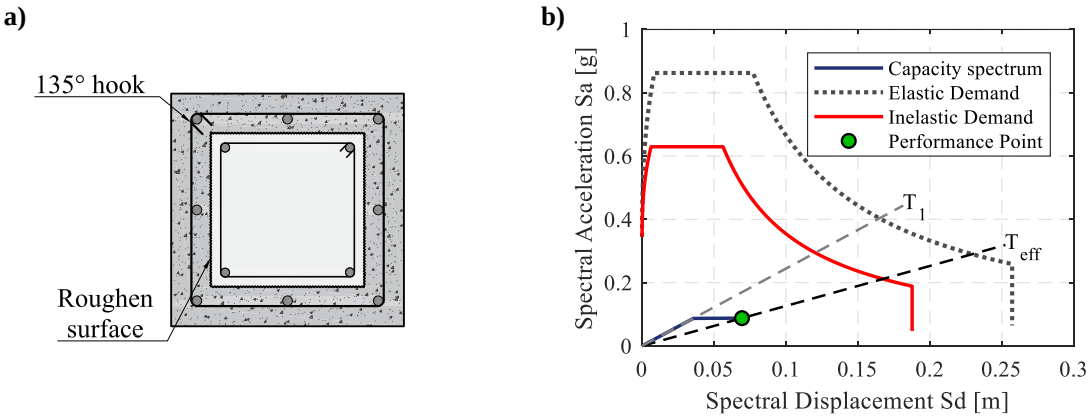

Figure 2. (a) a column retrofitted using RC jacketing; (b) as-built case: evaluation of CDR_{LS} using the CSM.

The iterative design process resulted in 17 retrofitted cases for RC jacketing. The layout, geometric details, and CDR_{LS} for a few example retrofit configurations are reported in Table 1. More configurations are described in Aljawhari et al. (2022). It is interesting to note that it was possible to achieve a CDR_{LS} up to 181% using RC jacketing as this strategy does not only improve ductility but also lateral strength and stiffness, making it capable of shifting the plastic mechanism to a global beam-sway one.

Table 1. Description of some configurations of retrofitted structures using RC jacketing.

Retrofit strategy	CDR_{LS} [%]	Description of the retrofit design/layout/geometry	Graphical illustration
RC Jacketing	65	Retrofit exterior columns on the 1st to 3rd floor with 50 mm jacket with 4Φ14 mm bars and 150 mm-spaced hoops.	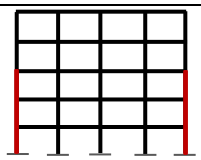
	105	50 mm jackets for the exterior columns on the 1st to 4th floor with 4Φ14 mm bars and 150 mm-spaced hoops. 50 mm jackets for the interior columns in 1st, 3rd, 4th floors with 4Φ16 mm bars and 150 mm-spaced hoops	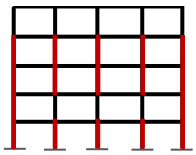
	181	On the 1st floor, 100 mm jackets with 8Φ16 mm bars for the exterior and 12Φ22 mm bars for interior columns, both with 100 mm-spaced hoops. 50 mm jackets with 8Φ20 mm bars for the exterior and 8Φ22 mm bars for the interior columns of the 2nd floor, both with 150-mm spaced hoops. 50 mm jackets with 8Φ14 mm bars and 150 mm-spaced mm hoops for the 3rd to 5th floors	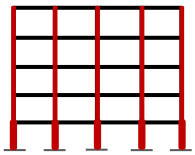

2.5 Derivation of Fragility Relationships

To compute seismic-damage EIs for the as-built and retrofitted configurations, it is first required to characterise the damage states (DSs) that may result from ground shaking. This is achieved using fragility relationships that define the probability of exceeding several DSs at various levels of a ground-shaking intensity measure (IM), i.e., $P(DS \geq DSi|IM)$. These relationships are expressed as standard normal cumulative distribution functions (∅) as per Eq. (1). μ_{DSi} and β are the median and dispersion for the "i-th" damage state (DSi), respectively. The adopted ground-shaking IM is the geometric mean of the 5%-damped spectral acceleration values over a pre-defined range of periods ($avgSa$). The $avgSa$ was computed considering ten equally-spaced periods between $0.2\mathrm{T}_1$ and $1.52\mathrm{T}_1$, where T_1 is the first-mode vibration period of the as-built structure.

$$P(DS \geq DSi|IM) = \Phi\left(\frac{\ln(IM/\mu_{DSi})}{\beta}\right) \quad (1)$$

Four different DSs are identified in this study: DS1 is for non-structural cracks. DS2 represents moderate structural and non-structural damage with no significant yielding. DS3 reflects extensive damage with some residual strength. DS4 indicates near-collapse conditions with fully exploited ductility and deficient residual strength. These DSs can be inferred numerically by measuring the maximum interstorey drift ratio (MIDR) from structural analysis and then comparing it with the MIDR thresholds corresponding to the onset of each DS. The derivation of fragility relationships for the as-built and retrofitted configurations was completed by Aljawhari et al. (2022) using the procedure of Jalayer et al. (2017). Figure 3a depicts examples of fragility relationships for the as-built and one of the retrofitted configurations. Figure 3b reports the variation of CDR_{LS} and the corresponding μ_{DSi} for all DSs to reflect the incremental improvement of seismic performance.

2.6 Definition of Seismic Hazard

The severity of EIs depends on the seismicity of the site of interest, which is characterised via hazard analysis, assuming the case-study frame is in L'Aquila, Italy (42.350 N°, 13.400 E°), among the seismically active areas in Italy. The soil type is C, with a shear-wave velocity of 270 m/s. The hazard is analysed via OpenQuake Engine (Pagani et al. 2014), adopting the 2013 Euro-Mediterranean Seismic Hazard Model (Giardini et al. 2014). The correlation model proposed by Baker and Jayaram (2008) is used and applied to all ground-motion models (GMMs) in the logic tree, except for the Akkar and Bommer (2010) GMM, where the Akkar et al. (2014) correlation model is used instead. Figure 4 shows the resulting hazard curves characterising a range of IM (i.e., $avgSa$) levels and their mean annual frequency of exceedance (λ).

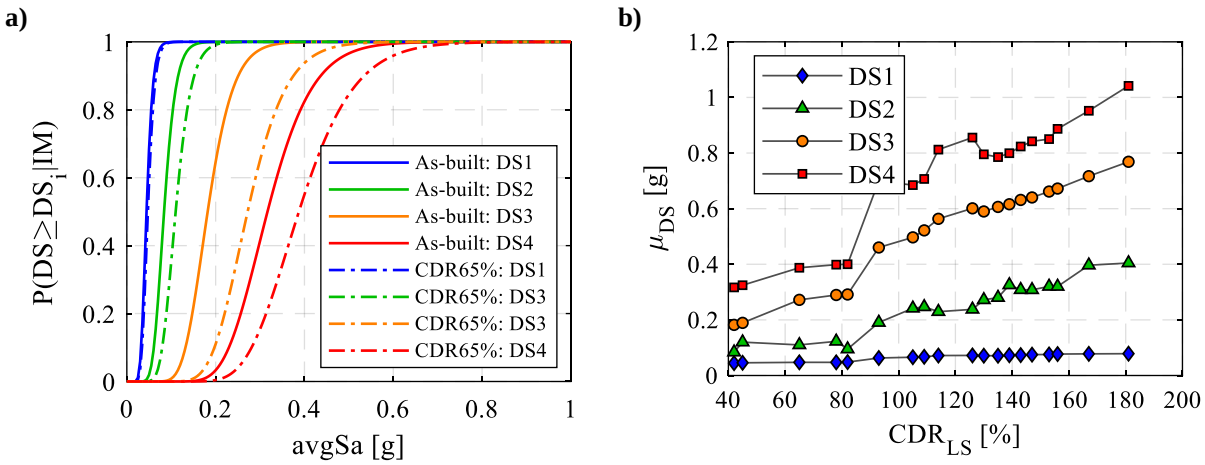

Figure 3. (a) examples of fragility relationships; (b) variation of CDR_{LS} versus μ_{DSi}.

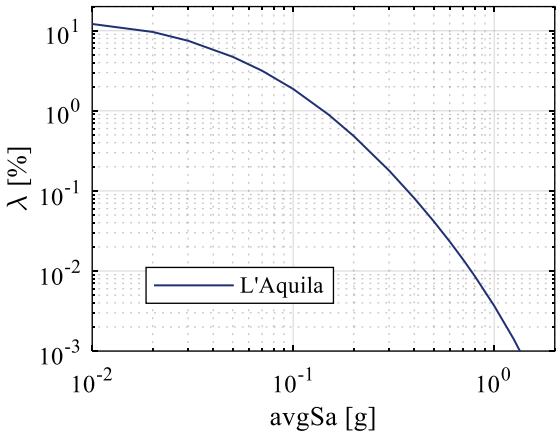

Figure 4. Seismic hazard curve for L'Aquila, Italy.

2.7 Earthquake-induced Environmental Impacts (EIs)

The EIs of seismic damage are expressed here in terms of embodied carbon, a metric that quantifies the total greenhouse emissions converted to equivalent kilograms (kgs) of carbon dioxide (CO_{2eq}). This metric is an indicator of global warming potential (and climate change) (e.g., Padgett and Li 2016). To estimate this metric at the building's level, it is first required to derive vulnerability functions defining the embodied carbon produced at different IM levels by combining the fragility relationships with suitable damage-to-embodied carbon ratios (DCO_2Rs). These ratios define the embodied carbon resulting when the building experiences a specific DS, normalised by its replacement embodied carbon. Eq. (2) shows the derivation of a mean vulnerability function, expressed as a ratio between the embodied carbon of seismic damage and that resulting from building replacement (CO_2R) over a range of IMs. The DCO_2Rs are acquired from past work by the authors on the numerical derivation of consequence models (Aljawhari et al. 2023), and they are summarised in Table 2.

$$CO_2R(IM) = \sum_{i=1}^{n} P(DS = DSi|IM)\, DCO_2Ri \tag{2}$$

Table 2. Adopted DCO_2Rs for different DSs and design-code levels.

Structure/DS	DS1	DS2	DS3	DS4
	DCO_2R1 [%]	DCO_2R2 [%]	DCO_2R3 [%]	DCO_2R4 [%]
5-storey pre-code	8.3	32.5	60.2	80.2
5-storey low-code	8.8	41.1	69.2	87.1
5-storey high-code	11.9	43.1	73.5	90.2

The embodied-carbon vulnerability functions in Eq. (2) are then combined with seismic hazard to acquire the so-called environmental loss curves that characterise the λ for any CO_2R values. These curves are finally integrated to compute the so-called expected annual embodied carbon (EAL_{CO2}), which constitutes a strong indicator of the average embodied carbon generated by seismic damage annually, as explained by Eq. (3). Table 3 reports the EAL_{CO2} values for both the as-built and retrofitted configurations. These values are greatly influenced by low DSs (DS1 and DS2) as they occur at relatively low IM levels, which have higher frequency. It should be noted that the EAL_{CO2} values are reported in both the normalised and absolute formats. The latter is obtained by multiplying the former with the building replacement embodied carbon ($ReCO_2$) obtained from Blengini (2009) and Aljawhari et al. (2023). Table 3 indicates that the reduction of EAL_{CO2} due to incremental retrofit is consistent as CDR_{LS} increases. The reduction of EAL_{CO2} becomes very pronounced at CDR_{LS}>90% as it the plastic mechanism of the building shifts from a column-sway to a global beam-sway mechanism.

$$EAL_{CO2} = \int_0^{\infty} CO_2R(IM)\, dIM \tag{3}$$

Table 3. EAL_{CO2} values for the as-built and retrofitted configurations assuming high hazard.

CDR [%]	$\boldsymbol{EAL_{CO2}}$ **[%]**	$\boldsymbol{EAL_{CO2}}$ $\boldsymbol{[kgCO_{2eq}]}$
42 (as-built)	1.330	8,295
45	1.309	8,164
65	1.130	7,048
78	1.030	6,424
93	0.694	4,328
105	0.582	3,630
109	0.561	3,499
114	0.544	3,393
126	0.531	3,312
130	0.502	3,131
135	0.494	3,081
139	0.455	2,838
143	0.458	2,857
147	0.447	2,788
153	0.436	2,719
156	0.427	2,663
167	0.394	2,457
181	0.387	2,414

2.8 Retrofit Intervention Environmental Impacts (EIs)

To understand the life-cycle impact of retrofit, it is further required to evaluate the embodied carbon generated during the implementation works of the retrofit strategy. Several methods can be adopted for such a purpose like the unit process (e.g., Welsh-Huggins et al. 2020) and economic input-output methods (Leontief 1986). This study uses the so-called embodied carbon factors (f_{CO_2eq}), which estimate the greenhouse gas emissions associated with the production of construction materials, expressed as kgs of CO_2eq per unit quantities (e.g., tons, m^2, m^3) (Hammond and Jones 2008) The overall embodied carbon is easily computed by multiplying each f_{CO_2eq} with the material quantity required for the construction activity.

The factors used here are obtained from Aljawhari et al. (2023), who derived them based on empirical data from various Italian manufacturers of construction materials and some of them are summarised in Table 4. These factors account only for the material production stage as it represents the largest share of emissions.

The effects of demolition, waste processing, and disposal are added separately assuming 3.4 $\mathrm{kgCO_2eq}$ per 1 m^2 for demolition and 0.013 $\mathrm{kgCO_2eq}$ for each 1 kg of material for waste processing and disposal (RICS 2017). It is also assumed that 90% of the waste materials are recycled (Napolano et al. 2015).

Table 4. Values of f_{CO_2eq} [in kgs of CO_2eq] for different construction materials, after Aljawhari et al. (2023)*.*

Product/material category	Average f_{CO_2eq}	Standard Deviation (σ)	Unit Quantity
Concrete	299.00	113.000	m^3
Steel reinforcement	729.00	94.000	ton
Sand (fines)	31.25	9.510	ton
Cement	733.75	132.130	ton
Clay bricks	0.24	0.056	kg
Epoxy resin	6.64	1.160	kg
Insulation for external walls	3.37	1.040	m^2
Wall paint	6.21	1.600	kg

To use the factors in Table 4, it is required to identify construction activities that could result in non-negligible emissions, as per Table 5, and then estimate the quantities of required materials. Activities such as technical efforts, scaffolding installation, and shoring are not incorporated due to their limited contribution to embodied carbon. The geometric variability of the retrofitted column is also addressed here to make the embodied carbon estimates of RC jacketing useful for future studies. Accordingly, it is assumed that column/beam dimensions and floor height as uniformly distributed random variables as explained in De Risi et al. (2020) and Aljawhari et al. (2023). The same treatment applies to the jacket's details. Specifically, the longitudinal rebar ratio (ρ_j) ranges between 0.3% and 1.5%, spacing between hoops (s_j) is between 50 and 150 mm, hoop diameter ($d_{s,j}$) is between 8 and 12 mm, and jacket thickness (t_j) ranges from 0.05 and 0.20 m. Accordingly, 10,000 samples of geometric parameters are sampled via a Monte Carlo approach. The variability of f_{CO_2eq} is also considered by generating another 10,000 samples based on the average and σ values in Table 4.

Table 5. Construction activities generating embodied carbon in the RC jacketing strategy.

Category	Activity Description
Infill walls next to the column	Re-building double-leaf infills via hollow bricks (external leaf is 12x25x25 cm and internal leaf is 8x25x25 cm)
	Adding mineral glass wool layer with a 30mm thickness for thermal insulation
	Plastering using a cement mortar applied in three layers on each side
	Painting surfaces using a three-layer water-based paint
Slab part around the column ends	Slab plastering work
	Painting the slab
	Adding a screed layer
	Laying floor tiles
Retrofit operations	Adding the steel cage (longitudinal rebar, hoops, and dowels)
	Create holes in the existing column to put the dowels and add epoxy resin
	Casting in-situ concrete mix
	Plastering the jacketed column
	Painting the jacketed column using a three-layer water-based paint
Disposal	Landfill and waste processing

The embodied carbon of retrofit intervention is finally estimated by multiplying the quantities of construction materials with the corresponding sampled f_{CO_2eq} values, considering all the simulated geometric combinations. A multiple linear regression is subsequently carried out on the generated data sample and Eq. (4) is derived, which measures the RC jacketing embodied carbon as a function of the jacket's geometric and reinforcement features. A dispersion equal to 0.302 can be used to address the variability. The embodied carbon produced by the RC jacketing intervention is reported in Table 6 for the retrofitted 17 configurations.

$$CO_{2,RC} = \sum_{i=1}^{n_{ext}} \left[662.3t_j + 3.12\rho_j - 0.062s_j + 1.95d_{s,j} + 274.3\right] h_j + \sum_{i=1}^{n_{int}} \left[661.4t_j + 3.13\rho_j - 0.065s_j + 1.97d_{s,j} + 369.6\right] h_j \quad (4)$$

Table 6. Embodied carbon of RC jacketing intervention for all the configurations.

CDR [%]	**Embodied Carbon [$\mathbf{kgCO_2eq}$]**
42 (as-built)	0
45	15,632
65	58,265
78	78,950
93	88,818
105	96,634
109	96,722
114	108,090
126	108,426
130	124,812
135	138,867
139	139,017
143	139,833
147	139,939
153	140,159
156	140,265
167	142,402
181	144,349

Figure 5 illustrates the embodied carbon produced by retrofit intervention, normalised by $\mathrm{ReCO_2}$, at different levels of CDR_{LS}. This parameter could be as low as 4% and may reach up to 25% at very large CDR_{LS}. It can be noticed in Figure 5 that there is a sharp increase in the embodied carbon of intervention as a result of incremental retrofitting, which is attributed to the newly added columns at each retrofitting configuration. Other retrofit strategies, such as steel jacketing, the number of retrofitted columns might be capped, even under incremental retrofitting, resulting in a gentler increase in the embodied carbon.

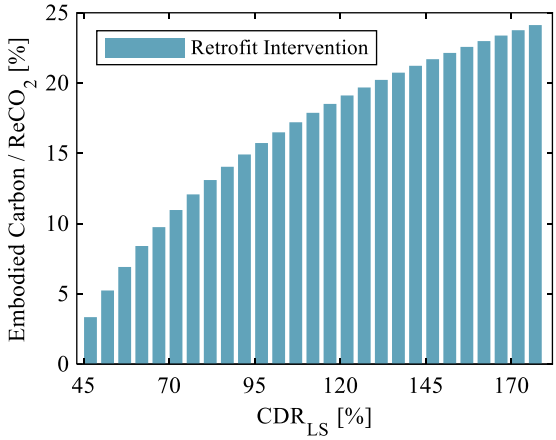

Figure 5. Retrofit embodied carbon divided by $ReCO_2$ at different CDR_{LS} values.

3 Results and Discussion

Upon evaluating the embodied carbon produced by the various retrofit interventions and that resulting from seismic damage, the overall life-cycle embodied carbon can be now estimated as per Eq. (5). C_{r,CO_2} is the retrofit embodied carbon and T is the building's remaining service life, assumed 50 years (e.g., Cardone et al. 2019). It is acknowledged that that such life-cycle is not comprehensive as it should ideally account for the embodied carbon related to the operation and maintenance stages. However, the contribution of these stages is almost identical in the as-built and retrofitted configurations, so it reasonable to disregard them when comparing seismic retrofit strategies/configurations. If the retrofit strategy includes energy upgrades (Caruso et al. 2021), then the operation and maintenance stages must be addressed in the building's life cycle.

$$Life\ cycle_{CO_2} = C_{r,CO_2} + T \cdot EAL_{CO_2} \cdot ReCO_2 \tag{5}$$

Figure 6a depicts the variation of life-cycle embodied carbon evaluated using Eq. (5) over the entire range of CDR_{LS}. The increase of C_{r,CO_2} and decrease of seismic embodied carbon due to incremental retrofit are also shown. A gradual reduction is observed in the life-cycle embodied carbon as CDR_{LS} increases until reaching an optimal value (the dashed line), which corresponds to a CDR_{LS} of 160%, which is quite larger than the basic performance objective (i.e., CDR_{LS} = 100%) stipulated by codes like Eurocode 8-3 (EN 1998-3 2005). Beyond the optimal CDR_{LS}, the life-cycle embodied carbon begins to increase again as the reduction in EAL_{CO_2} becomes trivial compared to the increase in C_{r,CO_2}. Figure 6b illustrates the percentage of difference between the life-cycle embodied carbon of the retrofitted configurations and the as-built structure. which indicates that a reduction of almost 40% can be achieved in the life-cycle embodied carbon at the optimal CDR_{LS}. However, the reduction is 26% if the retrofit configuration only satisfies the code requirement of CDR_{LS} equal to 100%.

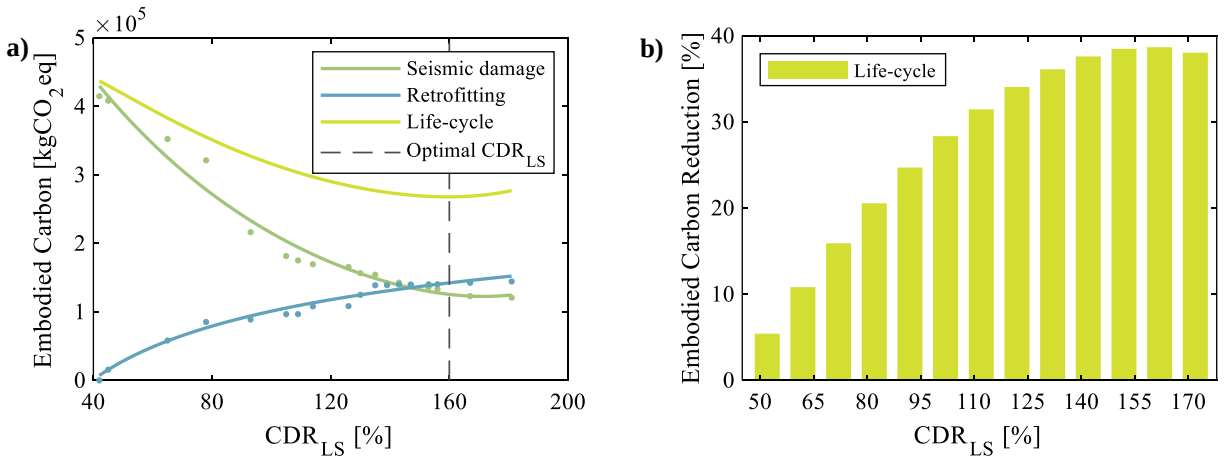

Figure 6. (a) life-cycle embodied carbon including seismic damage repair and retrofit intervention versus CDR_{LS}; (b) reduction in life-cycle embodied carbon due to retrofit intervention

Finally, to assess the real impact of seismic retrofit, the life-cycle embodied carbon obtained from Eq. (5) is compared to that associated with the initial construction of the building, as shown by Figure 7. The individual contributions of seismic damage over the building's service life and the retrofit interventions are also displayed in Figure 7. It can be noticed that the life-cycle embodied carbon of the as-built structure, which is caused only by earthquake-induced damage, constitutes nearly 70% of that emitted during initial construction. This number declines with incremental retrofit and becomes around 43% at the optimal CDR_{LS} level, with the contribution of seismic damage being less than 17%, whereas the remaining (i.e., 26%) is due to the retrofit intervention. Such a percentage might be even lower if the adopted retrofit strategy is more environmentally friendly than the RC jacketing, provided that it offers a similar improvement of seismic performance. This is because the embodied carbon of intervention in this study at large CDR_{LS} levels could be equally high, or even higher than that produced by seismic damage over the building's service life.

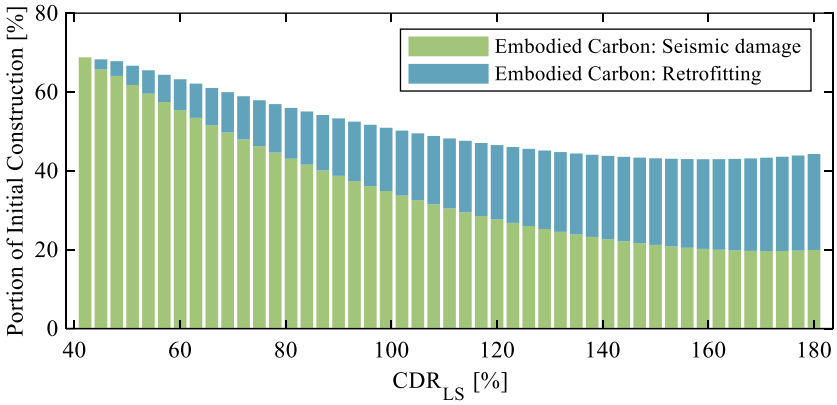

Figure 7. Life-cycle embodied carbon normalised by that related to the initial construction.

4 Remarks and Conclusions

This study investigated the influence of RC jacketing strategy on the life-cycle embodied carbon of a case-study non-ductile RC frame located in a highly seismic zone in Italy. 17 different configurations of retrofitted buildings were considered to account for different design choices. The life-cycle embodied carbon included a part induced by seismic damage, which was estimated by combining the fragility relationships of the as-built and retrofitted buildings with suitable damage-to-embodied carbon ratios, DCO_2Rs, developed by the authors in an earlier study. The other part represents the emissions generated due to retrofit interventions, which were computed by disaggregating the construction work into individual activities and evaluating the required material quantities. These were then multiplied with embodied carbon factors, f_{CO_2eq}, and aggregated to obtain the overall value. A simplified mathematical expression was also developed, which can be used by practitioners to measure the embodied carbon of retrofit intervention based on the geometric features of RC jacketing.

It was shown that the use of RC jacketing can achieve a significant reduction on life-cycle embodied carbon. The optimal reduction was equal to nearly 40% compared to the life cycle of the as-built structure. This took place at a CDR_{LS} equal to 160%, which is much larger than the Eurocode 8-3 objective (i.e., CDR_{LS} = 100%). On the other hand, satisfying the code minimum requirement offered less than 26% reduction compared to the as-built structure. The life-cycle embodied carbon was also compared to that related to the initial construction. It was shown that the embodied carbon caused by seismic damage reached almost 70% of that emitted during initial construction. In contrast, the optimal CDR_{LS} provided a substantially reduced embodied carbon at the life-cycle level that did not exceed 43%, with the seismic damage contribution being less than 17%. Future research efforts should consider different retrofit strategies that might be more environmentally friendly than RC jacketing, especially that the retrofit intervention using this strategy may generate embodied carbon that is larger than that resulting from seismic damage during the entire service life of the building under consideration.

5 References

Akkar, S., and J. J. Bommer. 2010. "Empirical Equations for the Prediction of PGA, PGV, and Spectral Accelerations in Europe, the Mediterranean Region, and the Middle East." *Seismological Research Letters*, 81 (2): 195–206. https://doi.org/10.1785/gssrl.81.2.195.

Akkar, S., M. A. Sandikkaya, and B. Ay. 2014. “Compatible ground-motion prediction equations for damping scaling factors and vertical-to-horizontal spectral amplitude ratios for the broader Europe region.” *Bulletin of Earthquake Engineering*, 12. https://doi.org/10.1007/s10518-013-9537-1.

Aljawhari, K., R. Gentile, and C. Galasso. 2022. “A fragility-oriented approach for seismic retrofit design.” *Earthquake Spectra*, 38 (3): 1813–1843. https://doi.org/10.1177/87552930221078324.

Aljawhari, K., R. Gentile, and C. Galasso. 2023. “Earthquake-induced Environmental Impacts for Residential Italian Buildings: Consequence Models and Risk Assessment.” *Journal of Building Engineering*. https://doi.org/doi.org/10.1016/j.jobe.2023.108149.

ATC. 1996. “40, Seismic evaluation and retrofit of concrete buildings.” *Applied Technology Council*, 1: 334.

Baker, J., and N. Jayaram. 2008. “Correlation of Spectral Acceleration Values from NGA Ground Motion Models.” *Earthquake Spectra - EARTHQ SPECTRA*, 24. https://doi.org/10.1193/1.2857544.

Blengini, G. A. 2009. “Life cycle of buildings, demolition and recycling potential: A case study in Turin, Italy.” *Build Environ*, 44 (2): 319–330. https://doi.org/10.1016/j.buildenv.2008.03.007.

Cardone, D., G. Gesualdi, and G. Perrone. 2019. “Cost-Benefit Analysis of Alternative Retrofit Strategies for RC Frame Buildings.” *Journal of Earthquake Engineering*, 23 (2): 208–241. https://doi.org/10.1080/13632469.2017.1323041.

Caruso, M., R. Couto, R. Pinho, and R. Monteiro. 2023. “Decision-making approaches for optimal seismic/energy integrated retrofitting of existing buildings.” *Front Built Environ*, 9. Frontiers Media SA. https://doi.org/10.3389/fbuil.2023.1176515.

Caruso, M., R. Pinho, F. Bianchi, F. Cavalieri, and M. T. Lemmo. 2020. “A life cycle framework for the identification of optimal building renovation strategies considering economic and environmental impacts.” *Sustainability (Switzerland)*, 12 (23): 1–20. https://doi.org/10.3390/su122310221.

Caruso, M., R. Pinho, F. Bianchi, F. Cavalieri, and M. T. Lemmo. 2021. *Integrated economic and environmental building classification and optimal seismic vulnerability/energy efficiency retrofitting*. *Bulletin of Earthquake Engineering*. Springer Netherlands.

Caterino, N., I. Iervolino, G. Manfredi, and E. Cosenza. 2008. “Multi-criteria decision making for seismic retrofitting of RC structures.” *Journal of Earthquake Engineering*, 12 (4): 555–583. https://doi.org/10.1080/13632460701572872.

EN 1998-1. 2004. *Eurocode 8: Design of structures for earthquake resistance - Part 1 : General rules, seismic actions and rules for buildings [Authority: The European Union Per Regulation 305/2011, Directive 98/34/EC, Directive 2004/18/EC]*. Brussels.

EN 1998-3. 2005. *Eurocode 8: Design of structures for earthquake resistance – Part 3: Assessment and retrofitting of buildings [Authority: The European Union Per Regulation 305/2011, Directive 98/34/EC, Directive 2004/18/EC]*. Brussels.

Gallo, W. W. C., G. Gabbianelli, and R. Monteiro. 2022. “Assessment of Multi-Criteria Evaluation Procedures for Identification of Optimal Seismic Retrofitting Strategies for Existing RC Buildings.” *Journal of Earthquake Engineering*, 26 (11): 5539–5572. Taylor & Francis. https://doi.org/10.1080/13632469.2021.1878074.

Gentile, R., and C. Galasso. 2021. “Simplified seismic loss assessment for optimal structural retrofit of RC buildings.” *Earthquake Spectra*, 37 (1): 346–365. https://doi.org/10.1177/8755293020952441.

Gonzalez, R. E., M. T. Stephens, C. Toma, and D. Dowdell. 2022. “The Estimated Carbon Cost of Concrete Building Demolitions following the Canterbury Earthquake Sequence.” *Earthquake Spectra*, 38 (3): 1615–1635. SAGE Publications Ltd STM. https://doi.org/10.1177/87552930221082684.

Gutiérrez- Urzúa, F., and F. Freddi. 2022. “Influence of the design objectives on the seismic performance of steel moment resisting frames retrofitted with buckling restrained braces.” *Earthq Eng Struct Dyn*, 51 (13): 3131–3153. https://doi.org/10.1002/eqe.3717.

Hammond, G. P., and C. I. Jones. 2008. “Embodied energy and carbon in construction materials.” *Proceedings of Institution of Civil Engineers: Energy*, 161 (2): 87–98. https://doi.org/10.1680/ener.2008.161.2.87.

Jalayer, F., H. Ebrahimian, A. Miano, G. Manfredi, and H. Sezen. 2017. “Analytical fragility assessment using unscaled ground motion records.” *Earthq Eng Struct Dyn*, 46 (15): 2639–2663. https://doi.org/10.1002/eqe.2922.

Leontief, W. 1986. *Input-Output Economics*. Oxford University Press, New York.

Liel, A. B., and G. G. Deierlein. 2013. “Cost-benefit evaluation of seismic risk mitigation alternatives for older concrete frame buildings.” *Earthquake Spectra*, 29 (4): 1391–1411. https://doi.org/10.1193/030911EQS040M.

De Luca, F., G. E. D. Woods, C. Galasso, and D. D’Ayala. 2018. “RC infilled building performance against the evidence of the 2016 EEFIT Central Italy post-earthquake reconnaissance mission: empirical fragilities and comparison with the FAST method.” *Bulletin of Earthquake Engineering*, 16 (7): 2943–2969. Springer Netherlands. https://doi.org/10.1007/s10518-017-0289-1.

McKenna, F. 2011. “OpenSees: A framework for earthquake engineering simulation.” *Comput Sci Eng*, 13 (4): 58–66. https://doi.org/10.1109/MCSE.2011.66.

Menna, C., M. C. Caruso, D. Asprone, and A. Prota. 2016. “Environmental sustainability assessment of structural retrofit of masonry buildings based on LCA.” *European Journal of Environmental and Civil Engineering*, 8189: 1–10. Taylor & Francis. https://doi.org/10.1080/19648189.2016.1232663.

Miano, A., H. Sezen, F. Jalayer, and A. Prota. 2017. “Performance-based comparison of different retrofit methods for reinforced concrete sructures.” *COMPDYN 2017 - Proceedings of the 6th International Conference on Computational Methods in Structural Dynamics and Earthquake Engineering*, 1: 1515–1535. https://doi.org/10.7712/120117.5510.17150.

Muntasir Billah, A. H. M., and M. Shahria Alam. 2014. “Performance-based prioritisation for seismic retrofitting of reinforced concrete bridge bent.” *Structure and Infrastructure Engineering*. Taylor & Francis.

Napolano, L., C. Menna, D. Asprone, A. Prota, and G. Manfredi. 2015. “LCA-based study on structural retrofit options for masonry buildings.” *International Journal of Life Cycle Assessment*, 20 (1): 23–35. https://doi.org/10.1007/s11367-014-0807-1.

Natale, A., C. Del Vecchio, and M. Di Ludovico. 2021. “Seismic retrofit solutions using base isolation for existing RC buildings: economic feasibilty and pay-back time.” *Bulletin of Earthquake Engineering*, 19 (1): 483–512. Springer Netherlands. https://doi.org/10.1007/s10518-020-00988-9.

NZSEE. 2017. *The Seismic Assessment of Existing Buildings, Part C5, Concrete Buildings*. New Zealand Society for Earthquake Engineering.

Padgett, J. E., and Y. Li. 2016. “Risk-Based Assessment of Sustainability and Hazard Resistance of Structural Design.” *Journal of Performance of Constructed Facilities*, 30 (2): 04014208. https://doi.org/10.1061/(asce)cf.1943-5509.0000723.

Pagani, M., D. Monelli, G. Weatherill, L. Danciu, H. Crowley, V. Silva, P. Henshaw, L. Butler, M. Nastasi, L. Panzeri, M. Simionato, and D. Vigano. 2014. “Openquake engine: An open hazard (and risk) software for the global earthquake model.” *Seismological Research Letters*, 85 (3): 692–702. https://doi.org/10.1785/0220130087.

Priestley, M. J. N., F. Seible, and G. M. Calvi. 1996. *Seismic Design and Retrofit of Bridges*. *Seismic Design and Retrofit of Bridges*.

RICS. 2017. “Whole life carbon assessment for the built environment: RICS professional statement, UK.” 41.

De Risi, M. T., C. Del Gaudio, and G. M. Verderame. 2020. *A component-level methodology to evaluate the seismic repair costs of infills and services for Italian RC buildings*. *Bulletin of Earthquake Engineering*. Springer Netherlands.

Rosti, A., C. Del Gaudio, M. Rota, P. Ricci, M. Di Ludovico, A. Penna, and G. M. Verderame. 2021. “Empirical fragility curves for Italian residential RC buildings.” *Bulletin of Earthquake Engineering*, 19 (8): 3165–3183. Springer Netherlands. https://doi.org/10.1007/s10518-020-00971-4.

Welsh-Huggins, S. J., and A. B. Liel. 2018. “Evaluating Multiobjective Outcomes for Hazard Resilience and Sustainability from Enhanced Building Seismic Design Decisions.” *Journal of Structural Engineering*, 144 (8): 04018108. https://doi.org/10.1061/(asce)st.1943-541x.0002001.

Welsh-Huggins, S. J., A. B. Liel, and S. M. Cook. 2020. “Reduce, Reuse, Resilient? Life-Cycle Seismic and Environmental Performance of Buildings with Alternative Concretes.” *Journal of Infrastructure Systems*, 26 (1): 04019033. https://doi.org/10.1061/(asce)is.1943-555x.0000510.